Dobslaw, H., Bergmann-Wolf, I., Dill, R., Poropat, L., Thomas, M., Dahle, C., Esselborn, S., König, R., Flechtner, F. (2017): A new high-resolution model of non-tidal atmosphere and ocean mass variability for de-aliasing of satellite gravity observations: AOD1B RL06. - *Geophysical Journal International*, *211*, 1, pp. 263—269.

DOI: http://doi.org/10.1093/gji/ggx302

Geophysical Journal International

Geophys. J. Int. (2017) **211,** 263–269
Advance Access publication 2017 July 19
GJI Gravity, geodesy and tides

doi: 10.1093/gji/ggx302

A new high-resolution model of non-tidal atmosphere and ocean mass variability for de-aliasing of satellite gravity observations: AOD1B RL06

H. Dobslaw, I. Bergmann-Wolf, R. Dill, L. Poropat, M. Thomas, C. Dahle, S. Esselborn, R. König and F. Flechtner

*Deutsches GeoForschungsZentrum—GFZ, Department 1: Geodesy, Telegrafenberg, D-*14473 *Potsdam, Germany. E-mail: dobslaw@gfz-potsdam.de*

Accepted 2017 July 18. Received 2017 July 14; in original form 2017 April 7

SUMMARY

The release 06 (RL06) of the Gravity Recovery and Climate Experiment (GRACE) Atmosphere and Ocean De-Aliasing Level-1B (AOD1B) product has been prepared for use as a time-variable background model in global gravity research. Available since the year 1976 with a temporal resolution of 3 hr, the product is provided in Stokes coefficients up to degree and order 180. RL06 separates tidal and non-tidal signals, and has an improved long-term consistency due to the introduction of a time-invariant reference orography in continental regions. Variance reduction tests performed with globally distributed *in situ* ocean bottom pressure recordings and sea-surface height anomalies from Jason-2 over a range of different frequency bands indicate a generally improved performance of RL06 compared to its predecessor. Orbit tests for two altimetry satellites remain inconclusive, but GRACE *K*-band residuals are reduced by 0.031 nm s^{-2} in a global average, and by more than 0.5 nm s^{-2} at numerous places along the Siberian shelf when applying the latest AOD1B release. We therefore recommend AOD1B RL06 for any upcoming satellite gravimetry reprocessing effort.

Key words: Global change from geodesy; Loading of the Earth; Satellite gravity.

1 INTRODUCTION

During the past 15 yr since the launch of the Gravity Recovery and Climate Experiment (GRACE; Tapley *et al.* 2004) in 2002 March, the concept of a low–low satellite-to-satellite tracking gravimetry mission has matured into a global monitoring system of mass redistribution and mass transport. Quantitative estimates of mass changes obtained from GRACE observations revealed, for example, substantial mass loss in the Tien Shan high-mountain glaciers (Farinotti *et al.* 2015); the non-sustainable depletion of groundwater resources in various densely populated regions of the world (Famiglietti 2014) and a gradually increasing Greenland meltwater discharge which impacts Labrador Sea convection and consequently the meridional overturning circulation in the North Atlantic (Yang *et al.* 2016). The relevance of GRACE for the monitoring of environmental changes is reflected in the approval of the follow-on mission GRACE-FO, which is scheduled for launch in Spring 2018 February (Flechtner *et al.* 2016).

Despite of its ability to accurately trace mass variability at large spatial scales, satellite gravimetry is inherently insensitive to discriminate between mass changes at, above, or beyond the Earth's surface. Further, the GRACE satellites are orbiting the Earth at an altitude of typically 450 km where small-scale features of the Earth's gravity field are already substantially diminished by the harmonic upward continuation. Gravity signals originating from processes that are sharply defined in the space domain, as, for example, mass loss of a single outlet glacier, are therefore smoothed into adjacent regions in the GRACE science products—an effect known as spatial leakage. Finally, GRACE is orbiting the Earth once every 90 min, and it requires the accumulation of data from various (typically 30) days to compute a full global gravity field. Signals at periods shorter than two times the accumulation period lead to spurious signals in the gravity field model—a phenomenon called temporal aliasing.

In order to aid the vertical signal separation problem and to reduce temporal aliasing, an *a priori* time-variable background model representing the mass variability in both atmosphere and oceans is typically introduced into the gravity field estimation procedure. The GRACE Atmosphere and Ocean De-Aliasing Level-1B (AOD1B) Product is routinely provided by Deutsches GeoForschungsZentrum (GFZ) since the launch date of the GRACE mission (Flechtner 2007; Flechtner *et al.* 2015). To meet its intended purposes, the product should fulfill two minimal requirements: (1) AOD1B needs to be provided with very high temporal and spatial resolution to properly represent transient weather systems and their associated pressure and mass signals. (2) AOD1B needs to be stable in time on long time-scales from years to decades in order to avoid the introduction of spurious low-frequency signals or discontinuities into the GRACE gravity fields that are subsequently prone to be interpreted erroneously in an entirely different geophysical context.

A detailed technical documentation of the latest AOD1B release 06 (RL06) is given in Dobslaw *et al.* (2016a). Besides

describing the processing strategy, this report also provides an assessment of the internal consistency of RL06 by analysing the time variability of AOD1B as represented both in spatial and spectral domains. Long-term trends in the re-synthesized atmospheric and oceanic components are well within the range of observed variability. Year-to-year changes do not reveal artificial low-frequency variations during the decades, and the assessment of specifically calculated 3 hr tendencies does not provide any indication for sudden jumps in the data. Consequently, the application of posterior corrections that account for occasional model changes at the European Centre for Medium-Range Weather Forecasts (ECMWF) present in the previous release 05 (RL05; Fagiolini *et al.* 2015) will not be necessary for any GRACE gravity field time-series utilizing AOD1B RL06.

In this study, we are going to contrast AOD1B mass variability from both RL05 and RL06 against a number of geodetic and oceanographic observations in order to assess its ability to represent high-frequency non-tidal mass variability for the purpose of reducing temporal aliasing effects. Since most high-frequency changes in AOD1B RL06 arise from the oceanic component as outlined in Section 2, we will concentrate on the validation with *in situ* ocean bottom pressure (OBP) observations (Section 3) and high-pass-filtered sea-level anomalies from radar altimetry (Section 4). Subsequently, the ability of both AOD1B versions to explain GRACE *K*-band residuals (Section 5) and to improve the precise orbit determination (POD) of two satellite altimetry missions (Section 6) are discussed, before a brief summary on the current quality level of AOD1B RL06 is presented.

2 OVERVIEW ON AOD1B RL06

The atmospheric component of AOD1B RL06 is based on ECMWF's re-analysis ERA-40 (Uppala *et al.* 2005) for 1976–1978; ERA-Interim (Dee *et al.* 2011) for 1979–2006; and the operational ECMWF analyses for all subsequent years. Surface pressure fields have been mapped onto a common reference orography as described in Dobslaw (2016). Upper air density effects that additionally modify the atmospheric gravity signal by up to 4 per cent are considered from the year 2000 onwards, since those signals are expected to be only relevant for low-earth orbiting missions equipped with Global Positioning System (GPS) receivers as pioneered by CHAMP (Reigber *et al.* 2002).

The oceanic component is based on an Max-Planck-Institute for Meteorology Ocean Model (MPIOM; Jungclaus *et al.* 2013) simulation with atmospheric forcing derived from ERA-40, ERA-Interim and operational ECMWF data, respectively, which is particularly less affected by secular trends in OBP that previously persisted in both AOD1B RL04 (Dobslaw & Thomas 2007) and RL05 (Dobslaw *et al.* 2013). Periodic signals associated with atmospheric tides and their corresponding oceanic responses have been fitted and removed for 12 of the most relevant frequencies in order to arrive at an AOD1B RL06 time-series that represents only the non-tidal mass variability in atmosphere and oceans. The latest release is given at 3 hr time-steps in terms of a spherical harmonic expansion complete up to degree and order (d/o) 100 and 180 before and after the year 2000, respectively. This increase in both temporal and spatial resolutions with respect to RL05 is motivated from the recent expansion of solution space of the GRACE monthly solutions (currently up to d/o = 96), and from the need to reduce interpolation artefacts induced when calculating gravity effects at arbitrary time epochs. All anomalies refer to a long-term mean calculated over the period 2003–2014 that approximately matches the length of one full solar cycle.

AOD1B RL06 is routinely updated at about 10 h UTC with all eight time-steps of the previous day. To potentially cover occasional data outages due to processing interruptions, we additionally provide a quick-look de-aliasing product based on the ECMWF deterministic forecasts with similar temporal but reduced spatial resolution (d/o = 50). Up-to-date information on status and quality of AOD1B including routinely updated statistics for low-degree coefficients is accessible at http://www.gfz-potsdam.de/en/esmdata (last accessed 12 July 2017). This website also provides information about non-tidal surface deformation model data sets compatible with AOD1B RL06 that might be used to consistently process Global Navigation Satellite Systems (GNSS) constellations or other space geodetic station data.

3 VALIDATION AGAINST *IN SITU* OCEAN BOTTOM PRESSURE OBSERVATIONS

We use a database of *in situ* OBP observations initially assembled by Macrander *et al.* (2010) containing station data sets from the time period 1998–2015 that vary in temporal resolution from 30 min to 24 hr. Starting from the raw pressure values at the original sampling, drift effects are removed by fitting a quadratic polynomial; jumps related to occasional sensor movements are corrected and episodic data outliers are identified and removed based on a 5σ criterion, which is applied in order to keep the number of data points flagged as outliers to the necessary minimum. Tidal signals are estimated and removed by means of the T_TIDE package for classical harmonic analysis (Pawlowicz *et al.* 2002). After removing the tides, data series from individual deployments at one station are stacked. Note that stacking is typically applied once every year, since most OBP recorders need to be lifted to the surface for battery replacement and general maintenance at regular intervals.

OBP observed from *in situ* sensors is contrasted against both AOD1B RL05 and RL06. A series of third-order Butterworth filters is applied to separate variability into three distinct frequency bands containing periods of 1–3, 3–10 and 10–30 d. The validation concentrates on the years 2004–2008 only where most *in situ* observations are available. Note that lower frequencies are not considered here since (i) uninterrupted *in situ* OBP observations are typically only available to us over time-spans of about 12–15 months; (ii) the contribution of barystatic sea-level changes not modeled by AOD1B increases at seasonal-to-interannual time-scales and (iii) the reliability of *in situ* observations decreases at longer periods due to sensor aging effects and resulting non-linear drifts in the station data.

To evaluate the AOD1B quality, we calculate the amount of variance of the *in situ* observations that is explained (or reduced) when AOD1B is subtracted. For the frequency band of 1–3 d, we note relatively poor performance of RL05 in the Arctic and in large parts of the Pacific (Fig. 1). AOD1B RL06 fits much better to the observations in those places, now explaining about 60 per cent of the variability at the North Pole. Less pronounced increases in explained variance for RL06 are also visible throughout most of the Pacific. In the Gulf of Alaska, however, RL06 performs slightly worse when compared to RL05. The overall consistency is rather low in that frequency band since both small timing errors in the onset of winds as represented by the atmospheric forcing data, or residual tidal variability at diurnal periods not properly removed from the *in situ* data degrade the fit between models and observations.

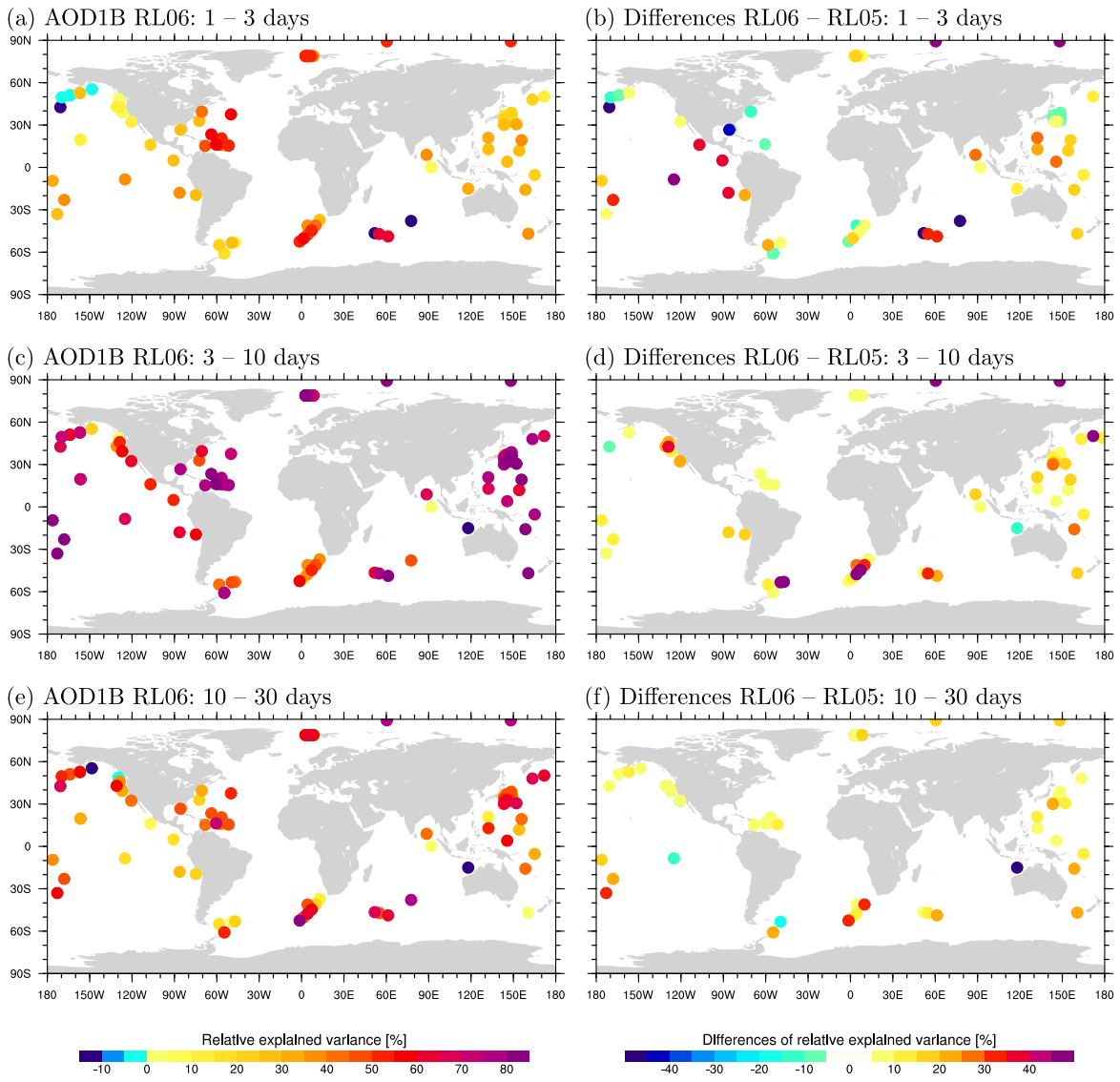

Figure 1. Relative variances (per cent) of *in situ* ocean bottom pressure observations explained by AOD1B RL06 (left-hand column) and differences between relative variances explained by RL06 and RL05 (right-hand column) that have been bandpass filtered for periods of 1–3 d (top row), 3–10 d (middle row) and 10–30 d (bottom row).

Improvements in RL06 are also apparent for the 3–10 d frequency band in particular in the Antarctic Circumpolar Current (ACC) region where ocean variability is strongly dominated by the surface wind forcing; and also in the Arctic Ocean, where the representation of ocean dynamics benefits most from the curvilinear horizontal grid utilized in MPIOM. For the longer periods between 10 and 30 d, we note a generally lower level of relative explained variances, since other dynamic processes apart from surface pressure and wind forcing have an increasing influence. Both RL05 and RL06 show an approximately similar fit to the *in situ* observations in that frequency range.

4 VALIDATION AGAINST JASON-2 SEA-LEVEL ANOMALIES

Sea-level variability as observed by radar altimetry missions is largely coherent with OBP changes at subseasonal time-scales away from the tropics (Bonin & Chambers 2011). In comparison to *in situ* OBP data which are only available from sparsely scattered locations, nadir-looking radar altimetry data are providing coverage for all ice-free oceanic regions over almost three decades now. We utilize four years of Jason-2 along-track sea-level data originating from the Jason-2 Geophysical Data Records, version D (GDR-D; CNES 2017) during 2012–2015 processed by GFZ's ADS Central (Schöne *et al.* 2010). The data are corrected for all recommended instrumental and geophysical effects as provided within GDR-D. For particular corrections, however, alternative models are applied, including solid Earth tides following the International Earth Rotation and Reference System Service (IERS) Conventions 2010 (Petit & Luzum 2010), and ocean and load tides (Savcenko & Bosch 2012). The commonly used dynamic atmospheric correction which combines a low-frequency inverted barometer (IB) effect with high-frequency signals from a barotropic ocean model is not applied. Instead, AOD1B-based OBP estimates are converted into sea-level

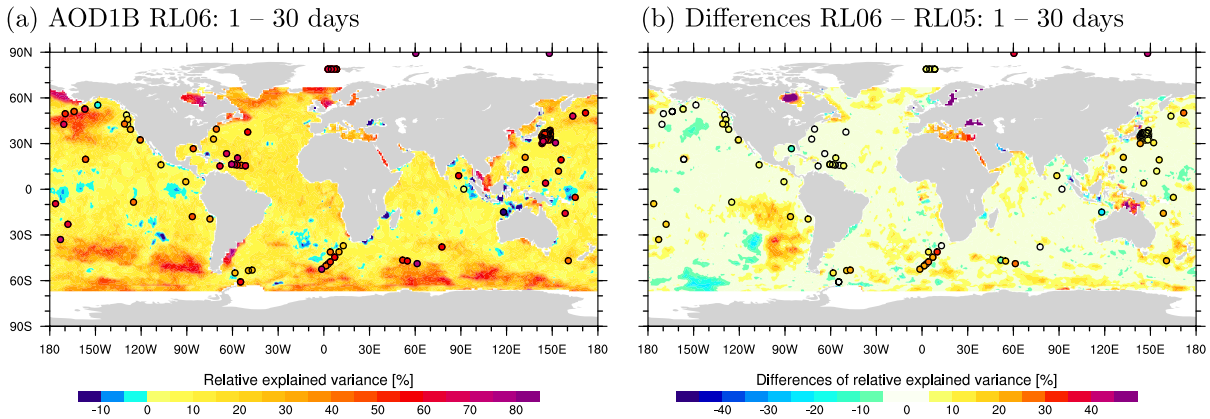

Figure 2. Relative variances (per cent) of sea-level variability from Jason-2 over the period 2012–2015 explained by (a) AOD1B RL06, and (b) differences between relative variances explained by RL06 and RL05, each bandpass filtered for periods of 1–30 d. For comparison, corresponding results from *in situ* ocean bottom pressure observations consistently filtered for identical frequencies are shown as well (circles). Note that *in situ* data were used from the years 2004–2008, which differs from the Jason-2 data period.

anomalies by using a mean sea-water density of 1028 kg m^{-3}, and are combined with the IB correction before being applied as an additional correction model to the Jason-2 along-track data. Residual daily sea-level anomalies are finally interpolated onto 1° equiangular grids using search radii of 300 km.

In order to focus on the high-frequency variability only, a third-order high-pass Butterworth filter with 30 d cut-off period is applied to the daily sampled Jason-based sea-level anomaly time-series from each gridpoint before calculating the variance fraction explained by AOD1B. For comparison, we also overlay relative explained variances of the *in situ* data that have been consistently bandpass filtered for periods between 1 and 30 d (Fig. 2). From this analysis, we note that both AOD1B versions reduce the variability in many regions, but patches of negative explained variance are substantially smaller for RL06. Clear improvements are in particular apparent in various semi-enclosed basins, as, for example, Hudson Bay, Baltic, Mediterranean, Red Sea and the Gulf of Carpentaria. For the Southern Ocean, we also identify large areas of improvement in particular in the Atlantic and Indian sectors of the ACC region, but note also some areas northwards of Ross Sea and Amundsen Sea where Jason-2 observed variability is better explained by RL05 than by RL06.

The level of explained variance is always slightly higher for *in situ* data when compared to Jason-2 observations, which is plausible since small but existing steric contributions to radar altimetry are neglected in our analysis, whereas the *in situ* OBP data are a direct measure of the quantity discussed here. We further note that the results of the two stations exhibiting negative skills for both RL05 and RL06 (located in the Gulf of Alaska and northwest off Australia) are not confirmed by the results of the radar altimetry, thereby suggesting that remaining errors in the processing of the *in situ* data as, for example, deficits in the reduction of tides might be responsible for the discrepancies found here. In general, however, both satellite altimetry and the *in situ* data support the conclusion that AOD1B RL06 is superior to RL05 in terms of reproducing the open-ocean high-frequency variability despite of the fact that largely different periods of data coverage are considered.

5 IMPACT ON GRACE K-BAND RESIDUALS

We also contrast both AOD1B versions with the primary sensor data of the GRACE mission, the *K*-band range-rate (KBRR) measurements between the two co-orbiting spacecraft performed by the intersatellite dual one-way microwave ranging instrument. We evaluate so-called KBRR pre-fit residuals that are obtained after data screening and POD of the GRACE satellites, but prior to the gravity field adjustment. Instrument data over the year 2008 are used here which are frequently applied as a test-case in GRACE data processing due to generally good data quality that benefits among other things from the low solar activity during that year. To pin-point the geographical location of an anomaly, KBRR residuals are transformed into *K*-band range acceleration (KBRA) residuals by differencing KBRR residuals in time followed by a fifth-order Butterworth low-pass filter with a cut-off frequency of 1/60 Hz. Individual KBRA residuals are binned into 3° boxes, and subsequently the variance of all KBRA residuals accumulated over the year in any particular box is calculated.

Since an improved modeling of forces acting on the GRACE satellites will result in a better fit between modeled and measured observations, a reduction of KBRA residual variance when moving from AOD1B RL05 to RL06 is interpreted as an improvement in RL06 over the previous version (Fig. 3). We note strong improvements with KBRA reductions of more than 0.5 nm s^{-2} (corresponding to roughly 25 per cent of the residual signal) over the Siberian Shelf, where artificial drifts were present in AOD1B RL05 that are now corrected in RL06. Variance reduction is also positive in the entire Arctic region and also in various semi-enclosed seas at the Northern Hemisphere including Hudson Bay, North Sea, Baltic and—less pronounced—the Mediterranean and the Black Sea, which are largely consistent with the results from Jason-2 presented above. Improvements are less clear in South-East Asia and in the ACC region, where numerous bins with even increasing KBRA residuals are documented. When looking at the global statistics, however, we note that the maximum improvement in any of the 3° boxes amounts to 2.241 nm s^{-2} (at 74°N, 161°E), the worst degradation is only to −0.488 nm s^{-2} (at 8°N, 104°E) and the global mean of 0.031 nm s^{-2} also supports the preference of RL06 over RL05.

6 IMPACT ON PRECISE ORBIT DETERMINATION

We finally test the impact of AOD1B on the POD of radar altimetry satellites. We essentially follow the processing strategy outlined in Rudenko *et al.* (2016), but focus on two satellites only that orbit

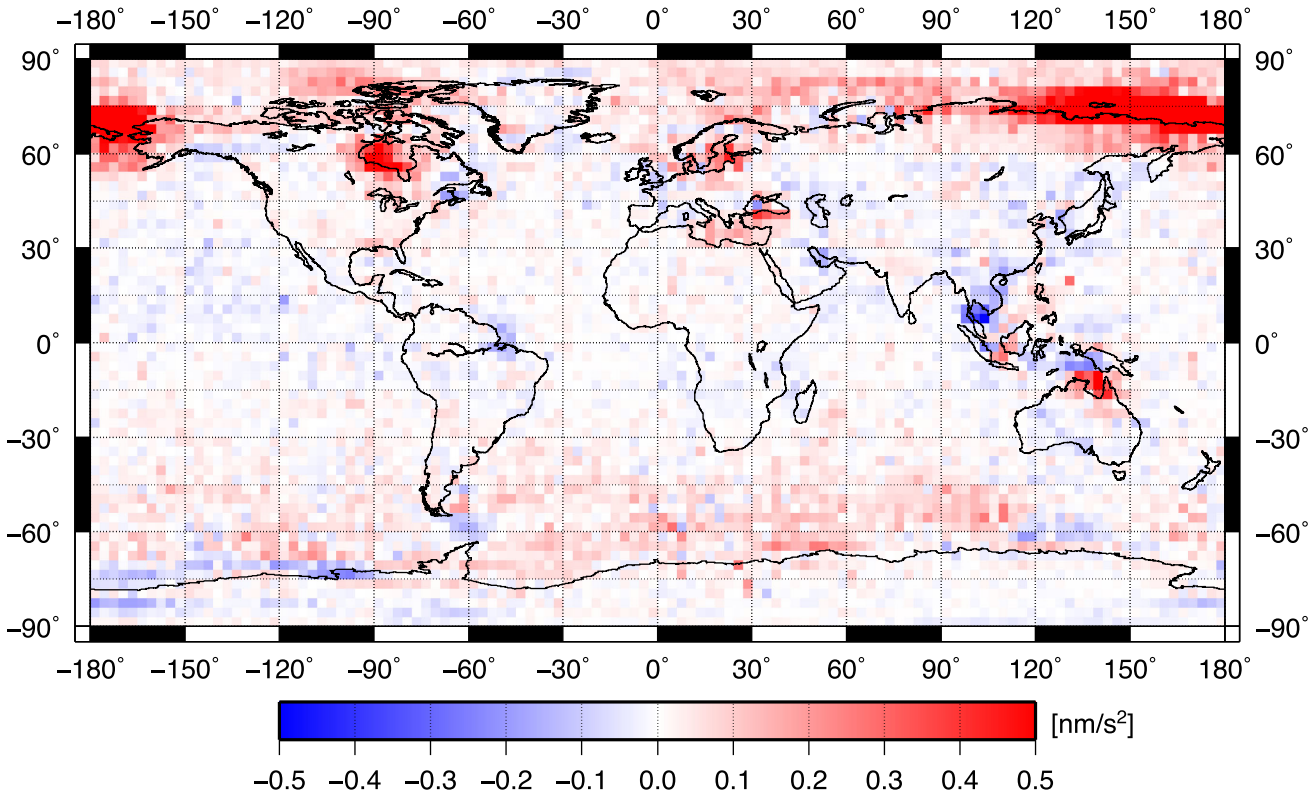

Figure 3. Reduction in GRACE *K*-band range acceleration residuals when replacing AOD1B RL05 with RL06 averaged over the year 2008.

Table 1. Impact of AOD1B RL05 and RL06 on precise orbit determination for the Jason-1 satellite as averaged over the period 2002–2012.

	SLR		DORIS	
AOD1B version	rms (mm)	Observation Count	rms (μm s^{-1})	Observation Count
RL05	15.12	1 767 916	357.2	46 050 097
RL06	15.11	1 767 916	357.2	46 050 097

Table 2. Impact of AOD1B RL05 and RL06 on precise orbit determination for the ENVISAT satellite as averaged over the period 2003–2012.

	SLR		DORIS	
AOD1B version	rms (mm)	Observation Count	rms (μm s^{-1})	Observation Count
RL05	12.92	1 026 514	428.8	32 460 082
RL06	12.94	1 026 514	428.7	32 460 081

the Earth at different altitudes and inclinations. Two versions of orbits have been computed for ENVISAT (2003–2012) and Jason-1 (2002–2012) by adding either AOD1B RL05 or RL06 to the time-variable background gravity field during the POD procedure. We utilize space geodetic observations of those satellites acquired from Satellite Laser Ranging (SLR) disseminated via the International Laser Ranging Service (Pearlman *et al.* 2005), and from the Doppler Orbitography and Radiopositioning Integrated by Satellite (DORIS) system provided via the International DORIS Service (Willis *et al.* 2010).

For every orbit version, individual *a posteriori* rms fits for each of the observation groups used for POD are calculated. Orbits of the Jason-1 satellite (1340 km altitude and 66° inclination) are just marginally improved both in terms of DORIS and SLR observations when AOD1B RL05 is replaced by RL06 (Table 1), the average improvements and their associated formal errors are small but significantly different from zero, that is, 0.009 ± 0.005 mm and 0.06 ± 0.02 μm s^{-1} for SLR and DORIS, respectively. SLR orbital fits for ENVISAT (800 km altitude and 98° inclination) slightly decrease when AOD1B RL05 is replaced by RL06 by -0.029 ± 0.008 mm (Table 2). For the DORIS observations, however, RL06 improves the fit with 0.039 ± 0.003 μm s^{-1}. Based on those numbers, we conclude that orbit tests are not a very sensitive option to assess the quality of present-day AOD1B modifications. Nevertheless, a small but positive impact of AOD1B RL06 is documented for almost all observation groups tested.

7 SUMMARY AND CONCLUSIONS

A new RL06 version of the de-aliasing product AOD1B has been calculated in preparation of the next reprocessing of monthly gravity fields from the GRACE satellite mission. Compared to its predecessor RL05, AOD1B RL06 provides an increased temporal (3 hr) and spatial (d/o = 180) resolution; a clear separation between tidal and non-tidal signals; and an improved long-term consistency due to the applied mapping of all atmospheric surface pressure fields to a time-invariant reference orography. Consequently, *a posteriori* correction models that account for occasional ECMWF model changes present in RL05 (Fagiolini *et al.* 2015) will be no longer necessary for a GRACE gravity field time-series utilizing AOD1B RL06.

Together with its predecessor, AOD1B RL06 has been tested for its ability to reduce scatter in four fundamentally different groups of oceanographic and geodetic observations that include *in situ* OBP station data, sea-level anomalies from satellite altimetry, GRACE *K*-band residuals as well as various space geodetic observations utilized for POD of Earth-orbiting satellites. Apart from rare

exceptions, AOD1B RL06 has been demonstrated to be superior over the previous release in all those assessments. In view of the additionally improved internal consistency of RL06 and the substantially reduced artificial drifts in the ocean component as documented in Dobslaw *et al*. (2016a), we recommend applying AOD1B RL06 for future reprocessing efforts of the GRACE observational record.

Model uncertainties relevant for temporal aliasing were previously analysed in detail for AOD1B RL05, and a 12-yr-long realization of realistic RL05-like errors was published as part of the updated Earth System Model of the European Space Agency (Dobslaw *et al.* 2015). Since uncertainties at periods longer than 30 d or occasional model change effects were never part of the error realization, we conclude that this error series is still approximately valid for satellite gravimetry simulation studies assuming GRACE RL06 error characteristics. A more refined quantification of the AOD1B RL06 contributions to temporal aliasing could be obtained from an update of a variance component estimation as given in table 2 of Dobslaw *et al*. (2016b), which will be, however, only possible as soon as multiyear series of time-variable gravity fields utilizing AOD1B RL06 are available.

In view of the results of Dobslaw *et al*. (2016b), we emphasize that even AOD1B RL06 is still about two times more accurate over the continents than over the oceans. Reasons for this are manifold and include the dense coverage of most continental regions with *in situ* atmospheric pressure sensors and the maturity of corresponding data assimilation techniques applied in numerical weather prediction; the general scarcity of meteorologic *in situ* sensors in open ocean regions away from the major commercial shipping routes that in particular include almost all polar and subpolar waters; the stronger variability of transient weather systems and its associated wind and surface pressure signatures over the open ocean; and the non-availability of high-frequency mass variability from global ocean state estimates as, for example, the ECMWF ocean re-analysis ORA-S4 (Balmaseda *et al.* 2013).

In a medium-term perspective, we therefore intend to continue working on alternative ocean model configurations to further improve the oceanic component of AOD1B. This includes testing the prospects of higher spatial and vertical resolution (von Storch *et al.* 2012); reconsidering self-attraction and loading feedbacks to ocean dynamics (Ray 1998; Kuhlmann *et al.* 2011); revisiting potential interactions between the general ocean circulation and the ocean tidal flow regime (Thomas *et al*. 2001; Li *et al.* 2015) and evaluating further modifications to the currently applied parametrizations of subgrid scale processes with the goal of improving the simulated bottom pressure variations in semi-enclosed seas, at the continental shelf, and in particular underneath the Antarctic ice shelves (Hellmer *et al.* 2012).

ACKNOWLEDGEMENTS

We are very grateful to the anonymous reviewer, Don Chambers, and the Editor Kosuke Heki for their insightful and comprehensive comments, which led to an improved representation of our results. We also thank Deutscher Wetterdienst, Offenbach, Germany, and the European Centre for Medium-Range Weather Forecasts (ECMWF), Reading, UK, for providing data from ECMWF's re-analyses and operational forecast models. MPIOM simulations were performed at Deutsches Klimarechenzentrum, Hamburg, Germany. This work has been funded by the German Federal Ministry of Education and Research (BMBF) within the FONA research program under grant 03F0654A.

REFERENCES

Balmaseda, M.A., Mogensen, K. & Weaver, A.T., 2013. Evaluation of the ECMWF ocean reanalysis system ORAS4, *Q. J. R. Meteorol. Soc.,* **139**(674), 1132–1161.

Bonin, J.A. & Chambers, D.P., 2011. Evaluation of high-frequency oceanographic signal in GRACE data: implications for de-aliasing, *Geophys. Res. Lett.,* **38,** L17608, doi:10.1029/2011GL048881.

CNES, 2017. *OSTM/Jason-2 Products Handbook,* CNES: SALP-MU-M-OP-15815-CN, EUMETSAT: EUM/OPS-JAS/MAN/08/0041, JPL: OSTM-29-1237, NOAA/NESDIS: Polar Series/OSTM J400(1), Rev. 11, 77 pp, Centre National D'Études Spatiales.

Dee, D.P. *et al.*, 2011. The ERA-Interim reanalysis: configuration and performance of the data assimilation system, *Q. J. R. Meteorol. Soc.,* **137**(656), 553–597.

Dobslaw, H., 2016. Homogenizing surface pressure time-series from operational numerical weather prediction models for geodetic applications, *J. Geod. Sci.,* **6,** 61–68.

Dobslaw, H. & Thomas, M., 2007. Simulation and observation of global ocean mass anomalies, *J. geophys. Res.,* **112**(C5), C05040, doi:10.1029/2006JC004035.

Dobslaw, H., Flechtner, F., Bergmann-Wolf, I., Dahle, C., Dill, R., Esselborn, S., Sasgen, I. & Thomas, M., 2013. Simulating high-frequency atmosphere-ocean mass variability for dealiasing of satellite gravity observations: AOD1B RL05, *J. geophys. Res.,* **118**(7), 3704–3711.

Dobslaw, H., Bergmann-Wolf, I., Dill, R., Forootan, E., Klemann, V., Kusche, J. & Sasgen, I., 2015. The updated ESA Earth System Model for future gravity mission simulation studies, *J. Geod.,* **89**(5), 505–513.

Dobslaw, H., Bergmann-Wolf, I., Dill, R., Poropat, L. & Flechtner, F., 2016a. *Product Description Document for AOD1B Release 06, Rev. 6.0*, 73 pp., GFZ Potsdam, Potsdam, Germany. Available at: ftp://isdcftp.gfz-potsdam.de/grace/DOCUMENTS/Level-1/GRACE_AOD1B_Product_Description_Document_for_RL06.pdf, last accessed 12 July 2017.

Dobslaw, H., Bergmann-Wolf, I., Forootan, E., Dahle, C., Mayer-Gürr, T., Kusche, J. & Flechtner, F., 2016b. Modeling of present-day atmosphere and ocean non-tidal de-aliasing errors for future gravity mission simulations, *J. Geod.,* **90**(5), 1–14.

Fagiolini, E., Flechtner, F., Horwath, M. & Dobslaw, H., 2015. Correction of inconsistencies in ECMWF's operational analysis data during de-aliasing of GRACE gravity models, *Geophys. J. Int.,* **202**(3), 2150–2158.

Famiglietti, J.S., 2014. The global groundwater crisis, *Nat. Clim. Change,* **4**(11), 945–948.

Farinotti, D., Longuevergne, L., Moholdt, G., Duethmann, D., Mölg, T., Bolch, T., Vorogushyn, S. & Güntner, A., 2015. Substantial glacier mass loss in the Tien Shan over the past 50 years, *Nat. Geosci.,* **8**(9), 716–722.

Flechtner, F., 2007. *AOD1B Product Description Document for Product Releases 01 to 04, Rev. 3.1*, 33 pp., GFZ Potsdam, Potsdam, Germany. Available at: ftp://isdcftp.gfz-potsdam.de/grace/DOCUMENTS/Level-1/GRACE_AOD1B_Product_Description_Document_for_RL01-RL04.pdf, last accessed 12 July 2017.

Flechtner, F., Dobslaw, H. & Fagiolini, E., 2015. *AOD1B Product Description Document for Product Release 05, Rev. 4.4*, 33 pp., GFZ Potsdam, Potsdam, Germany. Available at: ftp://isdcftp.gfz-potsdam.de/grace/DOCUMENTS/Level-1/GRACE_AOD1B_Product_Description_Document_for_RL05.pdf, last accessed 12 July 2017.

Flechtner, F., Neumayer, K.H., Dahle, C., Dobslaw, H., Fagiolini, E., Raimondo, J.C. & Güntner, A., 2016. What can be expected from the GRACE-FO laser ranging interferometer for Earth science applications?, *Surv. Geophys.,* **37**(2), 453–470.

Hellmer, H.H., Kauker, F., Timmermann, R., Determann, J. & Rae, J., 2012. Twenty-first-century warming of a large Antarctic ice-shelf cavity by a redirected coastal current, *Nature,* **485**(7397), 225–228.

Jungclaus, J.H. *et al.*, 2013. Characteristics of the ocean simulations in the Max Planck Institute Ocean Model (MPIOM) the ocean component of the MPI-Earth system model, *J. Adv. Model. Earth Syst.,* **5**(2), 422–446.

Kuhlmann, J., Dobslaw, H. & Thomas, M., 2011. Improved modeling of sea level patterns by incorporating self-attraction and loading, *J. geophys. Res.,* **116,** C11036, doi:10.1029/2011JC007399.

Li, Z., von Storch, J.-S. & Müller, M., 2015. The M 2 internal tide simulated by a 1/10° OGCM, *J. Phys. Oceanogr.,* **45**(12), 3119–3135.

Macrander, A., Boening, C., Boebel, O. & Schroeter, J., 2010. Validation of GRACE gravity fields by in-situ data of ocean bottom pressure, in *System Earth via Geodetic-Geophysical Space Techniques,* ed. Flechtner, F., pp. 169–185, Springer, Berlin.

Pawlowicz, R., Beardsley, B. & Lentz, S., 2002. Classical tidal harmonic analysis including error estimates in MATLAB using TDE, *Comput. Geosci.,* **28**(8), 929–937.

Pearlman, M. *et al.*, 2005. The International Laser Ranging Service and its support for IGGOS, *J. Geod.,* **40**(4–5), 470–478.

Petit, G. & Luzum, B., 2010. IERS Conventions 2010, *IERS Technical Note, 36,* Verlag Bundesamt fuer Kartographie und Geodäsie, Frankfurt, Germany.

Ray, R.D., 1998. Ocean self-attraction and loading in numerical tidal models, *Mar. Geod.,* **21**(3), 181–192.

Reigber, C. *et al.*, 2002. A high-quality global gravity field model from CHAMP GPS tracking data and accelerometry (EIGEN-1S), *Geophys. Res. Lett.,* **29**(14), 94–97.

Rudenko, S., Dettmering, D., Esselborn, S., Fagiolini, E. & Schöne, T., 2016. Impact of Atmospheric and Oceanic De-aliasing Level-1B (AOD1B) products on precise orbits of altimetry satellites and altimetry results, *Geophys. J. Int.,* **204**(3), 1695–1702.

Savcenko, R. & Bosch, W., 2012. *EOT11a—Empirical Ocean tide Model from Multi-mission Satellite Altimetry*. Available at: http://epic.awi.de/36001/1/DGFI_Report_89.pdf, last accessed 12 July 2017.

Schöne, T., Esselborn, S. & Rudenko, S., 2010. Radar Altimetry Derived sea level anomalies—the benefit of new orbits and harmonization, in *System Earth via Geodetic-Geophysical Space Techniques,* ed. Flechtner, F., pp. 317–324, Springer.

Tapley, B.D., Bettadpur, S., Watkins, M.M. & Reigber, C., 2004. The gravity recovery and climate experiment: mission overview and early results, *Geophys. Res. Lett.,* **31,** L09607, doi:10.1029/2004GL019920.

Thomas, M., Sündermann, J. & Maier-Reimer, E., 2001. Consideration of ocean tides in an OGCM and impacts on subseasonal to decadal polar motion excitation, *Geophys. Res. Lett.,* **28**(12), 2457–2460.

Uppala, S.M. *et al.*, 2005. The ERA-40 re-analysis, *Q. J. R. Meteorol. Soc.,* **131,** 2961–3012.

von Storch, J.-S., Eden, C., Fast, I., Haak, H., Hernández-Deckers, D., Maier-Reimer, E., Marotzke, J. & Stammer, D., 2012. An estimate of the Lorenz energy cycle for the World Ocean based on the STORM/NCEP simulation, *J. Phys. Oceanogr.,* **42**(12), 2185–2205.

Willis, P. *et al.*, 2010. The International DORIS Service (IDS): toward maturity, *Adv. Space Res.,* **45**(12), 1408–1420.

Yang, Q., Dixon, T.H., Myers, P.G., Bonin, J., Chambers, D. & van den Broeke, M.R., 2016. Recent increases in Arctic freshwater flux affects Labrador Sea convection and Atlantic overturning circulation, *Nat. Commun.,* **7,** 10525, doi:10.1038/ncomms10525.